Random and Aligned PLLA : PRGF Electrospun Scaffolds for Regenerative Medicine

Luis Díaz-Gómez,[1] Florencia Montini Ballarin,[2] Gustavo A. Abraham,[2] Angel Concheiro,[1] Carmen Alvarez-Lorenzo[1]

[1]Departamento de Farmacia y Tecnología Farmacéutica, Facultad de Farmacia, Universidad de Santiago de Compostela, 15872-Santiago de Compostela, Spain
[2]Instituto de Investigaciones en Ciencia y Tecnología de Materiales, Universidad Nacional de Mar del Plata-CONICET, Argentina
Correspondence to: C. Alvarez-Lorenzo (E-mail: carmen.alvarez.lorenzo@usc.es) and G. A. Abraham (E-mail: gabraham@fi.mdp.edu.ar)

ABSTRACT: Random and aligned electrospun scaffolds were prepared combining poly(L-lactic acid) (PLLA) and activated platelet-rich plasma (PRGF) at various proportions, with the aim of elucidating the role of nanofibers orientation and growth factors on cell attachment and proliferation. PRGF is released from scaffolds in a sustained way for at least 3 weeks, without an initial burst effect. Mesenchymal stem cells (MSCs) seeded on the random scaffolds present a polygonal and random orientation in any direction of the scaffold. On the other hand, aligned scaffolds are able to promote cell attachment and proliferation in the direction of the nanofibers. The incorporation of PRGF in the scaffolds enhances cell proliferation for at least 2 weeks. Overall, aligned electrospun PLLA : PRGF scaffolds can encapsulate growth factors at relatively large proportions and sustain their release to enhance cell attachment and proliferation as well as eliciting cell alignment. © 2014 Wiley Periodicals, Inc. J. Appl. Polym. Sci. **2015**, *132*, 41372.

INTRODUCTION

Electrospinning is a versatile technique to produce nanofibrous scaffolds from different natural and synthetic polymers, able to mimic the extracellular membrane matrix (ECM) morphology. Furthermore, it allows the use of different setups to obtain nanofibrous scaffolds with high porosity and high surface-to-volume ratio, with tunable pore and nanofiber diameter as well as different nanofiber orientation.[1–3] The nanofiber size and orientation, degradation rate and porosity affect the release kinetics of bioactive molecules included into them. These properties also determine the response of cells in contact with the scaffold.[4,5] Certain tissues, such as tendon or ligaments, require high mechanical resistance and therefore have an organized collagen-based fibrous structure to distribute the strength they are subjected to.[6] Bioreabsorbable synthetic polyesters, like poly(L-lactic acid) (PLLA), present a high Young modulus with a mechanical behavior similar to collagen, semicrystalline structure and good electro-spinnability.[7] PLLA is a safe, biodegradable polymer commonly used in biomedical applications, such as drug delivery systems, tissue engineering, and medical devices.[8–10] Random and aligned PLLA scaffolds have been prepared via electrospinning, solely or in combination with others. Aligned nanofiber PLLA can regulate the orientation of adhered cells.[11]

Electrospun scaffolds can be functionalized with bioactive molecules without changing bulk properties in order to improve tissue regeneration.[12] Immobilization of proteins (e.g., growth factors, GFs) on the scaffold surface improves cell-biomaterial interactions enabling modulation of cell recruitment, infiltration and scaffold colonization.[13] Electrospun scaffolds can also be used as reservoirs including bioactive molecules in the nanofibers as a way to control their release in the injured tissue.[14] GFs play a main role in tissue regeneration due to their ability to promote cell proliferation, differentiation and chemotaxis.[15] Incorporation of one or more GFs into scaffolds has been tested as a way to protect them from degradation and to provide sustained release at the injury site.[16,17] Most of studies deal with GFs obtained from recombinant sources, but the high costs and the difficulty of achieving physiologically relevant concentrations have prompted the search of new sources of GFs.[18] Platelets rich plasma (PRP) and its lyophilized powder (PRGF) are gaining attention as a natural, inexpensive, and ease-to-obtain source of GFs.[19–22] PRP enhances regenerative tissue response by complement activation, microvascular changes and endothelial proliferation, maintaining the physiological proportion in GFs.[13,22] PRP also contains other relevant bioactive molecules, such as fibrinogen, TSP-1 (trombospondin-1) or laminin-8, with a main role in cell-to-cell and cell-to-matrix

Table I. Electrospinning Parameters to Obtain Random and Aligned PLLA : PRP Scaffolds

Scaffold (PLLA : PRGF)	PLLA (%, w/v)	PRGF (%, w/v)	Voltage (kV)	Distance (cm)	Flow (mL/h)
10 : 0	10	0	15	10	0.5
10 : 1	10	1	15	10	0.5
10 : 3	10	3	15	10	0.5
10 : 5	10	5	15	10	0.5

interactions.[23,24] PRP has been already loaded in gelatin microspheres and alginate beads.[24,25] Electrospun scaffolds made of PRGF, alone or combined with biopolymers such as poly(ε-caprolactone) (PCL) or polyglycolic acid (PGA), were investigated to obtain implantable structures with better mechanical properties than hydrogel-based scaffolds. PRGF has been successfully incorporated into nanofiber scaffolds, resulting in a sustained release of active GFs over one month,[18] or adsorbed on scaffold surface creating a rich-in-GFs environment surrounding the implant.[26,27]

The aim of this work was to prepare random and aligned electrospun membranes combining PLLA and PRGF at various proportions, with the purpose of elucidating the synergistic effects that fiber orientation and GFs release may provide for regenerative medicine applications. The incorporation of PRGF into the scaffolds should enhance cell attachment and proliferation of mesenchymal stem cells (MSCs). Cell adhesion, proliferation and organization on mats prepared with various PLLA : PRGF weight ratios were evaluated.

EXPERIMENTAL

Materials
Poly(ʟ-lactic acid) (PLA2002D, Mw 287.9 KDa) from Natureworks (Minnetonka, MN); dichloromethane (DCM) and *N,N*-dimethylformamide (DMF) from Anedra (Buenos Aires, Argentina); phosphate-buffered saline (PBS, pH 7.4) from Sigma-Aldrich (St. Louis, MO); human adipose-derived stem cells (MSC) StemPRO® from Gibco (Life Technologies, Carlsbad, CA); and Pierce™ BCA (bicinchoninic acid) Protein Assay Kit from Thermo Scientific (Waltham, MA). All other reagents were analytical grade.

Platelet-Rich Plasma Preparation
Human buffy coat was obtained from healthy donors at the Galician Transfusion Center (Spain) and centrifuged for 15 min at $400 \times g$. The upper fraction containing high platelet concentration (PRP) was collected. Platelets were activated through freeze ($-80°C$)-thaw ($20°C$) cycles (once a day, 4 days) to allow the release of GFs from alpha and dense granules. Then, PRP was centrifuged at $12,000 \times g$ for 10 min at $4°C$ to separate growth factors-containing plasma from remnant platelets. VEGF concentration was measured by means of an enzyme-linked immunosorbent assay (ELISA) (RayBiotech, USA). Supernatant was frozen at °80°C and lyophilized, and the obtained dry powder (preparation rich in growth factors, PRGF) kept at 80°C until use.

Electrospinning of PRGF–PLLA Scaffolds
PLLA and PRGF solutions in DCM : DMF (60 : 40 v/v) were prepared to have 10% w/v PLLA[28] and 0, 1, 3, and 5% w/v

PRGF. DCM and DMF are common solvents used for electrospining of proteins.[29] Intrinsic solution properties and setup parameters for each PRGF concentration were first optimized to obtain bead-free fibrous membrane (Table I). A classic flat collector was used to obtain random electrospun membranes. PLLA : PRGF solution (5 mL) was charged in a syringe and electrospun for 6 h to obtain a mat of $\sim$250 μm thickness. Resulting scaffolds were dried under vacuum and kept at 4°C until use. A second setup was used to obtain well-aligned nanofibrous scaffolds. Two dielectric boards were placed over the collector plate to allow fiber deposition between the boards and also between the smaller board and the plate in a well-aligned morphology (Scheme I).

Scaffold Characterization
Micrographs of the PLLA : PRGF scaffolds (after sputter-coating with gold) were recorded in a scanning electron microscope (JSM-6460LV; JEOL, Japan) and processed using Image-Pro Plus software (Media Cybernetics, USA) to obtain the diameter and orientation of 100 nanofibers per sample. Water contact angles (5 μL droplet) on dry scaffold pieces were measured with a Ramé-Hart goniometer (Succasunna, NJ; 40 measures in 30 s). DSC analyses were carried out with a Pyris 1 (Perkin-Elmer; USA) instrument, heating at 10°C/min from 20 to 200°C under nitrogen atmosphere, and glass transition, crystallization, and melting events characterized. Crystallinity was estimated from melting and crystallization enthalpies calculated taking into account the PLLA mass in each sample, divided by PLLA 100% crystalline melting enthalpy. FTIR spectra in attenuated total refractance (ATR) mode were recorded over a range of 450–4000 cm^{-1} at a resolution of 2 cm^{-1} using Nicolet 6700 (Nicolet Instruments Inc., WI).

Protein Release
Electrospun scaffolds were cut as disks of 12 mm in diameter, sterilized in ethanol (80% v/v), rinsed three times in phosphate buffered saline (PBS) and placed in 24-well plates. Each well was filled with 1 mL of PBS and incubated at 37°C and 5% CO_2. At days 1, 3, 7, 11, and 21, the medium was collected and the wells refilled with PBS. Aliquots were kept frozen at $-80°C$ until analysis. Bicinchoninic acid (BCA) assay was used to quantify total protein release from scaffolds. Calibration curve was obtained from bovine serum albumin (BSA) solutions up to 2 mg/mL.

MSC Proliferation
Scaffold pieces (disks of 132 mm²) were placed in 24-well plates, sterilized in ethanol (80% v/v), rinsed three times in PBS and preincubated in culture medium, prepared with MesenPro RS (96%), MesenPro growth supplement (2%), glutamine (1%),
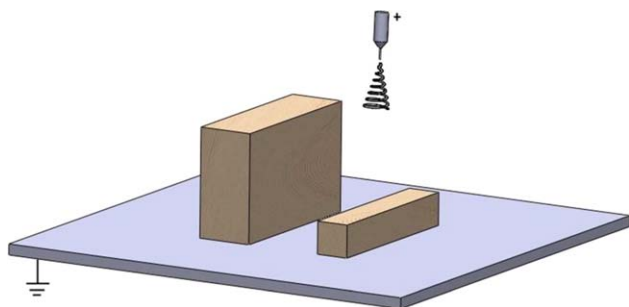
Scheme I. Setup used to obtain well-aligned electrospun fibers. Two dielectric boards placed over the collector plate allowed fiber deposition between the boards and also between the smaller board and the plate in a well-aligned morphology. The dimensions of the higher board were 8x8x4 cm and of the smaller board 3x8x4 cm, and the distance between them was 8 cm. [Color figure can be viewed in the online issue, which is available at wileyonlinelibrary.com.]

and antibiotics (penicillin-streptomycin; 10,000 units/mL and 10,000 μg/mL, respectively) (1%) overnight. MSCs were seeded on each scaffold at a concentration of $2 \cdot 10^4$ cells/well in 200 μL of medium and allowed to attach for 25 min. Then, 1 mL of culture medium was added in each well. Pyrex glass rings (12 mm inner diameter, 13.9 mm external diameter, 4.2 mm high, ca. 370 mg weight) were used to avoid scaffold flotation and shrinkage. Cells were cultured for 14 days on PLLA : PRGF scaffolds. MSCs proliferation was quantified at Days 1, 3, 7, and 14 using MTT assay (Roche, Switzerland). Briefly, scaffolds were incubated with the MTT reagent at 37°C for 4 h and then

overnight with the detergent included in the kit. Final solutions were collected and read at 550 nm (UV Bio-Rad Model 680 microplate reader, USA). All experiments were carried out in triplicate.

### Evaluation of Cell Morphology and Cytocompatibility

MSCs ($2 \cdot 10^4$ cells/scaffold) were cultured on the aligned and random scaffolds in 24-well plates, as described above. MSCs seeded on both random and aligned scaffolds after 7 days in culture were fixed in paraformaldehyde (4% in PBS) followed by dehydration in ethanol (70% v/v). Scaffolds were mounted, sputter-coated with gold, and observed using SEM (Zeiss Ultra Plus, Germany). Live-dead staining was also performed to analyze scaffold cytocompatibility and cell morphology. MSCs cultured in PLLA : PRGF scaffolds for 7 days were rinsed with PBS and stained with calcein (1 mg/mL) : propidium iodide (1 mg/mL) : PBS 2 : 1 : 97 vol/vol solution. After incubation in darkness for 10 min, cell morphology and viability were evaluated from images obtained using laser confocal fluorescence microscopy (LCS, Leica Microsystems, Germany). Confocal micrographs of the calcein staining (green color, live cells cytoplasm) were processed with ImagePro Plus software (Media Cybernetics, USA) to measure the cytoplasm orientation angle. At least 300 cytoplasms were measured per micrograph in order to obtain a meaningful statistical value.

Statistical Analysis

All data were expressed as mean ± standard deviation. t-Test was used to compare the fibers mean diameters, cell
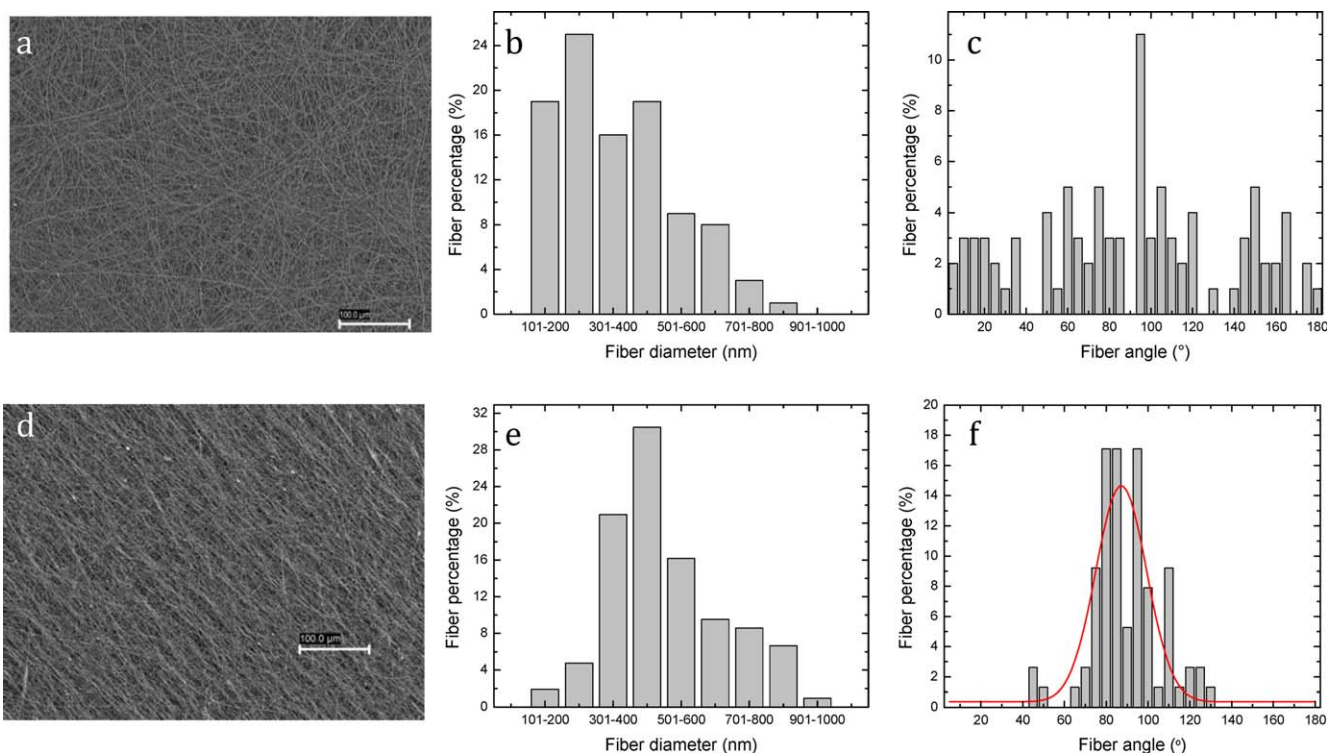
Figure 1. SEM micrographs and results of nanofiber topography analysis on random (a, b, c) and aligned (d, e, f) PLLA : PRGF 10 : 0 scaffolds. [Color figure can be viewed in the online issue, which is available at wileyonlinelibrary.com.]
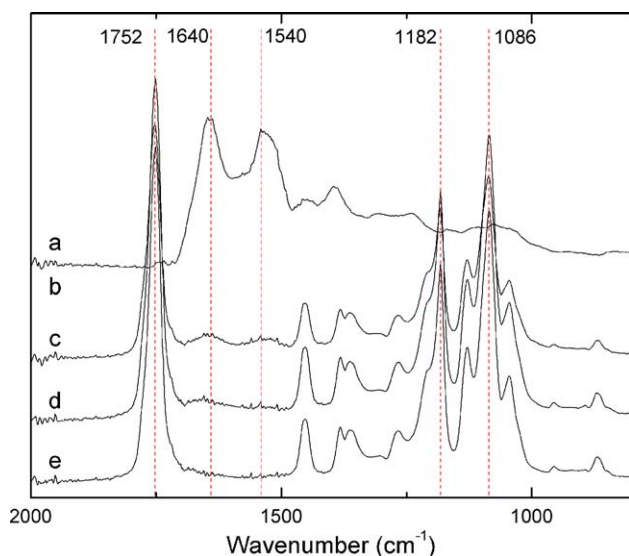
Figure 2. FTIR spectra of PRGF powder (a), and PLLA : PRGF 10 : 5 (b), 10 : 3 (c), 10 : 1 (d), and 10 : 0 (e) fibers. [Color figure can be viewed in the online issue, which is available at wileyonlinelibrary.com.]

proliferation, and PRGF release results of scaffolds prepared with and without PRGF ($\alpha < 0.05$).

RESULTS AND DISCUSSION

Preparation of Electrospun Fibers

PRP was successfully obtained from buffy coat, a concentrate rich in platelets.[30] After soft-conditions centrifugation, PRP was recovered from the upper section of the centrifuge tubes and aliquoted. Platelet concentration was $3.2 \cdot 10^6$ per μL, a value 10–15 times higher than blood levels. Concentration of VEGF, one of the most important growth factors contained in platelets was also measured, resulting in 116.2 pg/mL. This value was 12 times higher than blood levels in a healthy human. Freeze-thaw cycles have been previously demonstrated as a cost-effective technique capable of activate platelets.[31] Furthermore, subsequent freeze-drying process to make a dry powder from platelets lysate (PRGF) protects growth factors from degradation, with no loss of activity.[27]

Random and aligned electrospun nanofibers were obtained from solutions with different concentrations in PLLA and PRGF. The nature of the solvents and the processing parameters
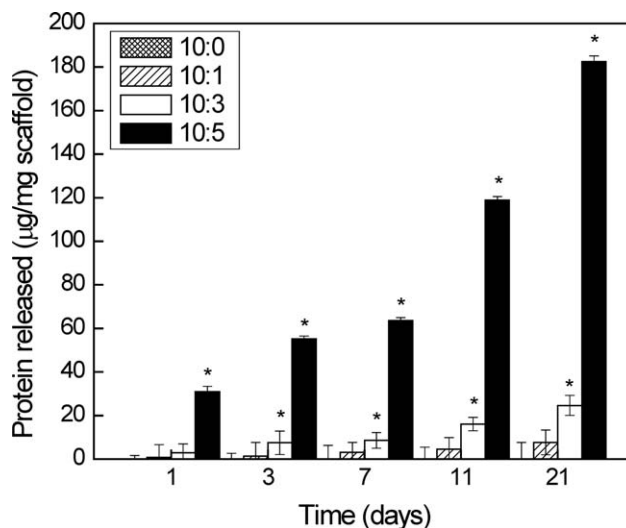
Figure 3. Cumulative amount of proteins released from PLLA : PRGF scaffolds in PBS at 37°C. *Statistically significant difference ($\alpha < 0.05$).

(voltage, needle-to-collector gap, injection speed) were adjusted for different PRGF concentrations (0, 1, 3, and 5 % wt/v) in order to obtain bead-free, continuous fibers as observed using SEM [Figure 1(a,b)]. PLLA : PRGF 10 : 0 random scaffolds presented a mean nanofiber diameter of 360 ± 174 nm. The incorporation of PRGF in the scaffolds resulted in mean fiber diameters of 402 ± 182 nm, 354 ± 119 nm, and 339 ± 147 nm for PLLA : PRGF 10 : 1, 10 : 3, and 10 : 5, respectively. The image processing results showed no change ($\alpha < 0.05$) in the fiber diameter as PRGF concentration increased. These results were in agreement with a previous report on PRGF incorporation in electrospun nanofibers prepared with silk fibroin, poly(-glycolic acid) or poly-ε-caprolactone, using 1,1,1,3,3,3 hexafluoro-2-propanol (HFP) as solvent.[18]

PLLA : PRGF solutions were also used to obtain well-aligned nanofibrous membranes. The dielectric boards setup resulted in parallel nanofibers with small deviations ($\pm 20°$) from the main direction (for plotting purposes, the angle measurements were normalized to 90°; namely, 90° means no deviation from the main direction) [Figure 1(c,f)]. Although the standard deviations were not small, all samples presented a unimodal histogram that corroborated that the nanofibers were oriented in nearly the same direction. In the case of random fibers, those oriented in the 80–100° interval only represent

Table II. Glass Transition (T_g), Crystallization (T_c), and Melting (T_m) Temperatures, Crystallization (ΔH_c), and Melting (ΔH_m) Heats, and Percent Crystallinity (X_c) for the Raw PLLA and PLLA : PRGF Electrospun Scaffolds

Scaffold (PLLA : PRGF)	T_g (°C)	T_c (°C)	ΔH_c (J/g)	T_m (°C)	ΔH_m (J/g)	X_c (%)[a]
PLLA raw	61.4	–	–	152.5	35.00	37.6
10 : 0	56.1	81.8	10.86	153.9	30.52	21.1
10 : 1	51.9	76.3	11.74	151.0	32.37	22.2
10 : 3	50.7	77.5	2.93	155.9	17.77	15.9
10 : 5	48.6	77.2	14.58	146.8	28.21	14.6
PRGF	–	–	–	–	–	–

[a] Values obtained assuming that ΔH_m PLLA 100% crystalline = 93 J/g.[35]
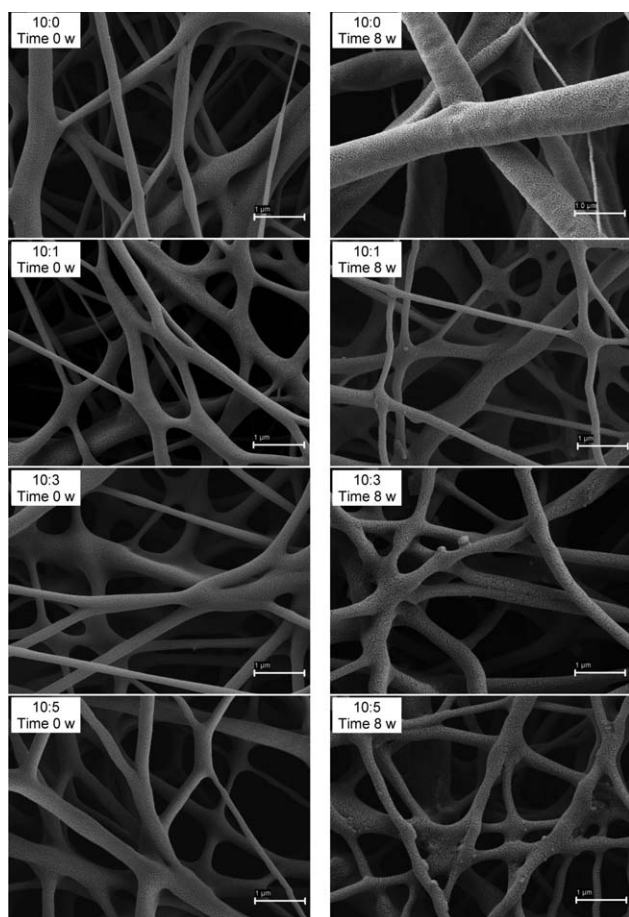
Figure 4. SEM micrographs of PLLA : PRGF electrospun scaffolds before (left) and after (right) incubation for 8 weeks in PBS at 37°C.

17% of the whole population [Figure 1(c)], compared with 64% in the case of aligned membranes [Figure 1(f)]. The aligned fibers presented a mean diameter of 487 ± 167 nm, which was greater than for random scaffolds ($\alpha < 0.05$), but still in the nanometer range. The increment in fiber diameter could be due to differences in the microjet time of flight. Although needle-collector distances were the same in both setups, the aligned fibers were collected over the dielectric board which surface is 8 cm above the collector plate. Therefore, the aligned fibers had a smaller time of flight, which reduced the microjet stretching, producing nanofibers with a slightly greater diameter.

FITR spectra of PRGF showed the characteristic amide I and II peaks of proteins at 1644 and 1534 cm^{-1}, respectively (Figure 2). These peaks, which were absent in the PLLA : PRGF 10 : 0 spectrum, appeared in the PLLA : PRGF 10 : 1, 10 : 3, and 10 : 5 scaffolds; the higher the PRGF proportion in the scaffolds, the higher the intensity of the peaks. This finding indicates that the incorporation of PRGF in the electrospun scaffolds was successful. FTIR spectra of the scaffolds also showed the carbonyl peak at 1752 cm^{-1} and C—O stretching at 1086 and 1182 cm^{-1}, which are characteristic of PLLA.

Glass transition (T_g), crystallization (T_c), and melting (T_m) temperatures, heat of crystallization (ΔH_c) and melting (ΔH_m), and crystallinity (X_c) of the fibers were analyzed by means of DSC (Table II). Raw PLLA thermographs showed glass transition at

61.4°C and melting at 152.5°C. Electrospinning led to a decrease in PLLA crystallinity. As reported before,[32] during the electrospinning process the solution solvent is rapidly evaporated and the polymer chains do not have enough time to accommodate in the crystalline structure; therefore, a more amorphous polymer is obtained. Crystallization peaks were observed in the DSC runs of electrospun fibers at 73–81°C. T_g also decreased due to the electrospinning. This finding can be attributed to the nanoscale confinement of the polymer chains,[33–35] as observed in nanometric polymer films.[36] It has been previously demonstrated that the T_g of amorphous nanofibers decreases with decreasing fiber diameter,[36] and consequently electrospun nanofibers have lower T_g than the raw material. PRGF incorporation decreased more the T_g, which indicates the intercalation of protein components among the polymer chains, acting as plasticizers.

Contact angle measurements evidenced that PLLA : PRGF 10 : 0 scaffolds were highly hydrophobic, resulting in a water drop angle of 126°. Similar results were obtained after water drop deposition on the surface of the PLLA : PRGF 10 : 1 and 10 : 3 scaffolds, where contact angle resulted in 122° and 124°, respectively. In contrast, PLLA : PRGF 10 : 5 scaffolds absorbed the water drop in a few seconds, which can be attributed to the greater concentration in hydrophilic proteins. Duan et al.[37] have previously shown that hydrophilization of surface scaffolds improves cell adhesion.

Protein Release

Total protein released from PLLA : PRGF scaffolds was monitored for up to 3 weeks in PBS at 37°C, by means of BCA assay (Figure 3). Degradation of PLLA fibers was not shown to affect protein quantification using BCA kit. Detectable amounts of proteins were released from PLLA : PRGF 10 : 1, 10 : 3, and 10 : 5 scaffolds already in the first 24 h, although only the latter scaffolds let to protein levels remarkably greater than the control ($\alpha < 0.05$). The more intense release was observed for the 10 : 5 scaffolds at the first days due to the presence of more
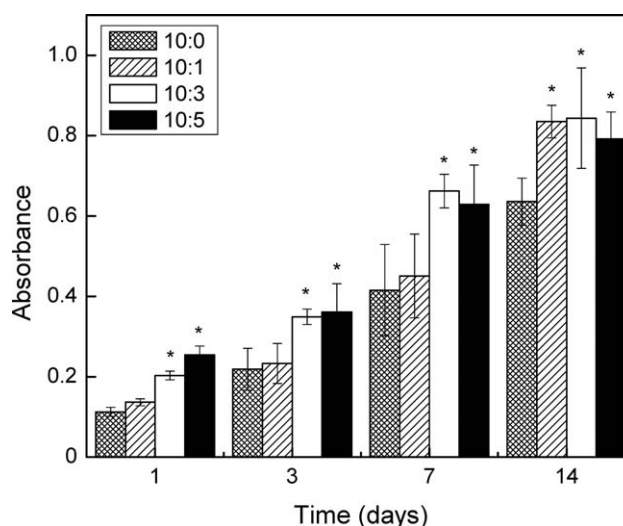
Figure 5. MSC proliferation on PLLA : PRGF scaffolds determined using MTT assay. *Statistically significant difference ($\alpha < 0.05$).
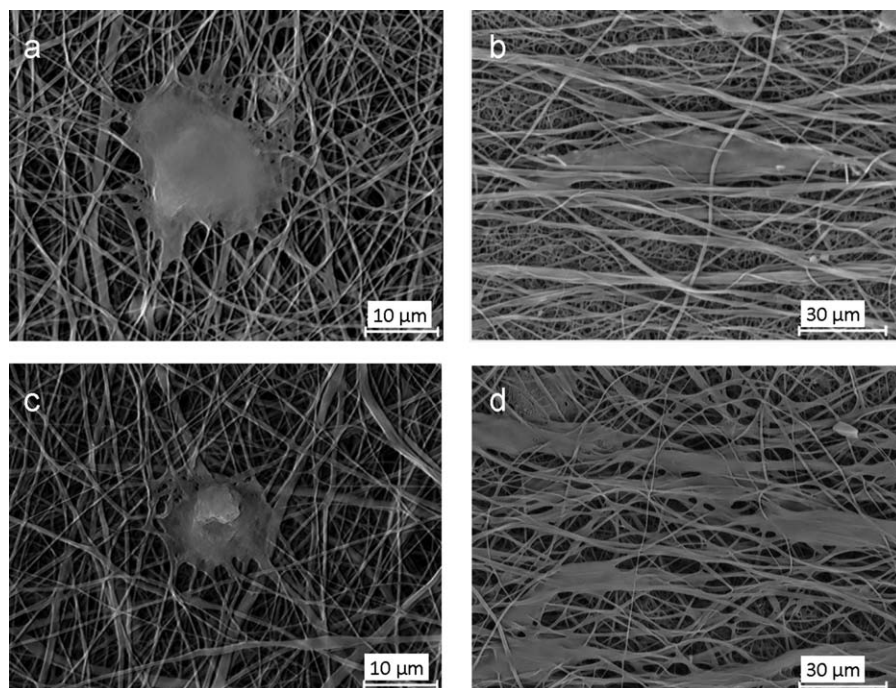
Figure 6. SEM micrographs of MSCs seeded on random (a, c) and aligned (b, d) PLLA : PRGF 10 : 0 (up) and 10 : 1 (below) scaffolds. Scale bars: 10 μm (left) and 30 μm (right).
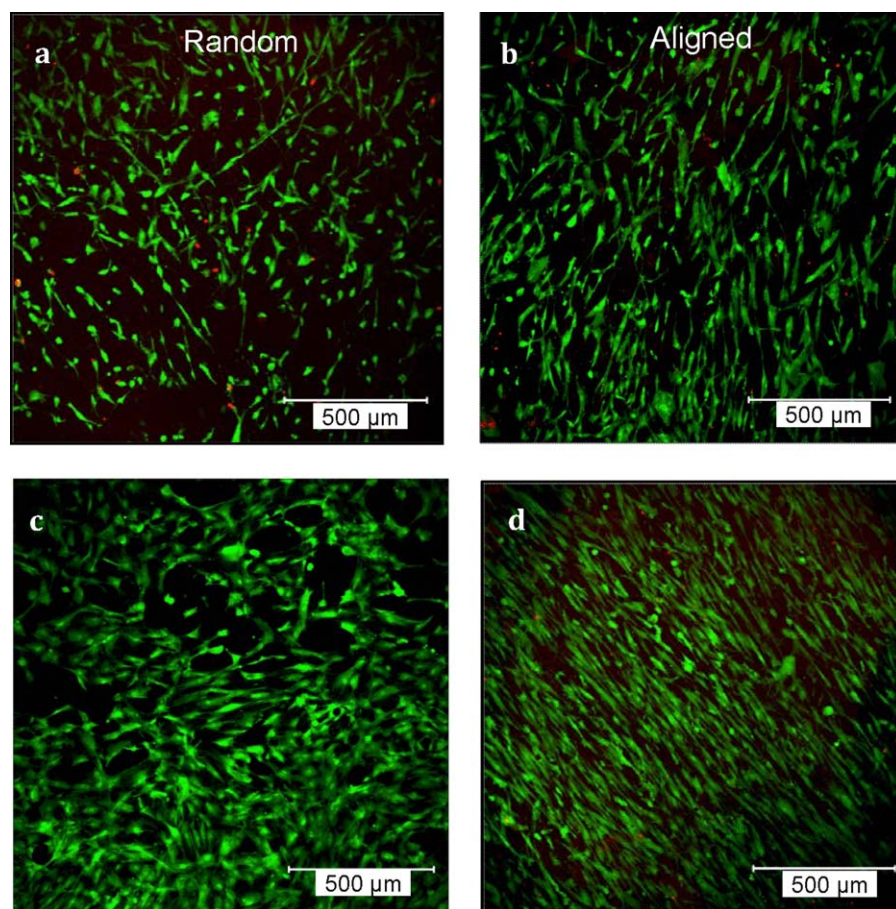
Figure 7. Live-dead staining of cells grown on random (a, c) and aligned (b, d) PLLA : PRGF 10 : 0 (up) and 10 : 5 (down) scaffolds after 7 days in culture (scale bar: 500 μm). [Color figure can be viewed in the online issue, which is available at wileyonlinelibrary.com.]
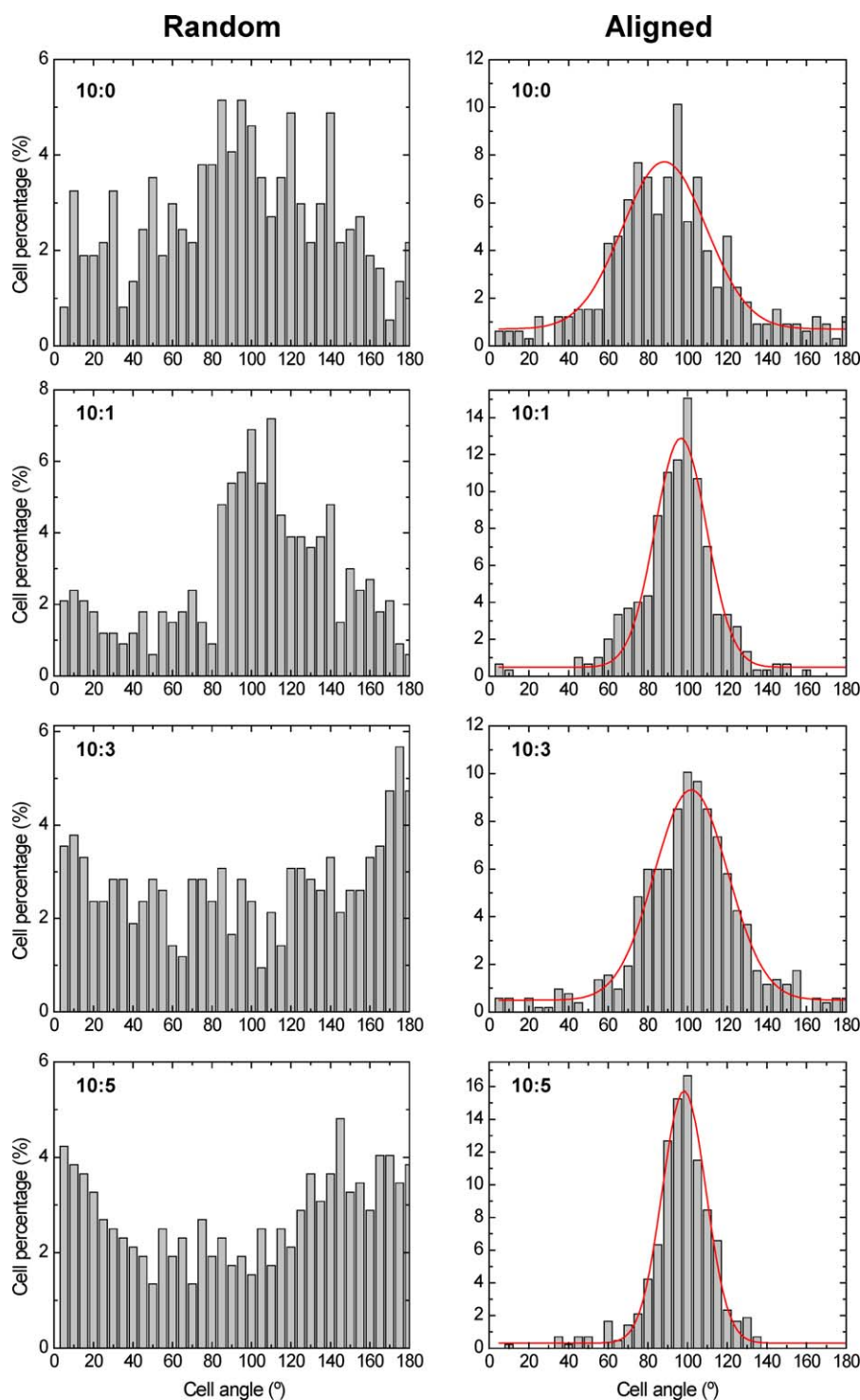
Figure 8. Quantification of cell orientation on random (left) and aligned (right) scaffolds. Values represent mean direction of cytoplasms stained with calcein. Angle dispersion is narrower when cells are oriented. [Color figure can be viewed in the online issue, which is available at wileyonlinelibrary.com.]

amounts of PRGF on or close to the fibers surface. Protein release slowed down between days 3 and 7, which can be associated to a lapse of time between the release of proteins from the scaffold surface and the sustained release from the bulk of the bioerodible scaffold. Protein released correlated to PRGF amount in the scaffolds. The release pattern showed by the

scaffolds is similar to those previously reported by Berkland et al.[38] for macromolecules release from biodegradable microspheres, which typically consist of three phases: an initial burst, an interval of slow release, and a final phase of faster release. Taken into account that PRGF has a total content in protein of 80%,[27] PLLA : PRGF 10 : 1, 10 : 3, and 10 : 5 contained ∼72,

184, and 266 μg protein per mg of scaffold. PLLA : PRGF 10 : 5 scaffolds released of up to 180 μg per mg of scaffold after 21 days; namely, 67.7% payload. PLLA : PRGF 10 : 3 scaffolds released 24.6 μg protein per mg of scaffold; that is, 13.4% payload. In the case of PLLA : PRGF 10 : 1 scaffolds, the release was about 11% at Day 21. Similar release profiles were observed for aligned fibers (data not shown).

Faster release from PLLA : PRGF 10 : 5 scaffolds compared to the other two ones is explained by changes in bulk structure above a certain PRGF proportion. Differently from PLLA, PRGF is hydrophilic and dissolves as water gets access to the scaffold inner structure. As observed from water contact angle measurements, scaffolds with PRGF weight contents of 9% and 23% (PLLA : PRGF 10 : 1 and 10 : 3, respectively) behave as hydrophobic, which means that those contents in protein cause minor changes in the bulk structure of PLLA matrix and that the proteins are well intercalated among the PLLA chains. Therefore, after release of the most accessible proteins, PLLA network efficiently prevent the access of release medium into the bulk until PLLA degradation occurs. Conversely, in the scaffolds with content in PRGF of 33.3% (PLLA : PRGF 10 : 5), there is an excess of protein to be encapsulated by PLLA matrix. PLLA scaffolds did not significantly erode in the 21 days of the study (Figure 4).[39] Thus, faster release is related to (almost) direct access of the proteins to the release medium. As observed in SEM micrographs of scaffolds taken after 8 weeks in release medium, only PLLA : PRGF 10 : 5 fibers showed changes in surface topography.

Analysis of Cell Proliferation

The effect of PLLA : PRGF random scaffolds on MSCs proliferation is shown in Figure 5. MSCs seeded on PLLA : PRGF 10 : 0 and 10 : 1 scaffolds showed similar growth up to 7 days in culture, which could be related to the fact that 10 : 1 scaffolds released too small amounts of PRGF during that period. Scaffolds with greater contents in PRGF notably enhanced MSCs growth ($\alpha < 0.05$). Both PLLA : PRGF 10 : 3 and 10 : 5 scaffolds led to a greater cell proliferation after 7 days. The reason of this similitude in cell proliferation could be due to the contact inhibition of the cells.[40] This phenomenon occurs when the cells are proliferating in a limited area and they encounter others as they are proliferating, inhibiting cell growth. In the present case, cells seeded on 10 : 5 scaffolds proliferated faster than those seeded on 10 : 3 scaffolds, activating earlier this mechanism. Differences in cell density were narrowed after 14 days in culture, probably due to the fact that cells attached to PLLA : PRGF 10 : 3 and 10 : 5 scaffolds became confluent.

As expected, scaffolds cytotoxicity was low, due to good biocompatibility of PLLA[41] and autologous PRGF.[42] Cytocompatibility results could be extrapolated from random to aligned scaffolds as previously found by Baker and Mauck[43] and discussed in next section.

Evaluation of Cell Morphology and Cytocompatibility

Morphology of MSCs seeded on aligned and random nanofiber scaffolds was visualized using SEM and confocal microscopy. MSCs attached to PLLA : PRGF scaffolds were able to assume different morphologies upon interaction with random or aligned scaffolds (Figure 6). Cells seeded on random nanofibers

were attached to the scaffolds without specific orientation. Conversely, cells adopted an elongated morphology in the same direction of the aligned nanofibers when cultured on oriented scaffolds. Random and aligned scaffolds presented similar fiber diameter; thus, observed differences in cell morphology can be attributed to the different topography. Confocal images also showed the morphology assumed by MSCs when cultured on random or aligned scaffolds (Figure 7). It was also observed that the scaffolds with high concentration in PRGF resulted in an increase in cell density.

Cell angle orientation on random and aligned PLLA : PRGF scaffolds was determined by measurement of cells cytoplasm on each scaffold using ImagePro Plus software (Figure 8). Cytoplasms orientation angles of the MSCs seeded on random scaffolds presented a wide distribution, indicating a high disparity in cell elongation. By contrast, cells seeded on aligned scaffolds showed narrow distribution of cell orientation angles, which indicate that cells remained oriented in the main direction of the nanofibers after 7 days in culture. Cell orientation differences were maintained until cell confluence on the scaffolds, in agreement with previous studies on aligned topographies using MSCs.[44,45] Integrin binding ligands, lamellipodia and filopodia, seem to be the clue to the topographical-mediated cell alignment.[46] Fiber organization promoted cell orientation through contact guidance, which is improved when nanofiber diameter is close to 300 nm. This topography facilitated the formation of a continuous monolayer of cells on the scaffolds.[47]

CONCLUSIONS

PRGF can be added at large proportions into PLLA electrospun nanofibers in a simple, cost-effective and reproducible way. Incorporation of PRGF up to 33.3% w/w does not significantly increases fiber diameter, but decreases the T_g and the water contact angle of the electrospun fibers. PLLA : PRGF scaffolds sustain protein release for more than 3 weeks, showing faster release those prepared with the greatest proportion in PRGF. PRGF notably promotes cell adhesion and proliferation on the scaffolds, while the alignment of fibers modulates cell orientation. Compared with PLLA and random PLLA : PRGF mats, aligned PLLA : PRGF scaffolds *in vitro* promoted cell alignment and elongation while enhancing cell attachment and proliferation.

ACKNOWLEDGMENTS

REFERENCES

1. Reneker, D. H.; Yarin, A. L.; Zussman, E.; Xu, H. *Adv. Appl. Mech.* **2007**, *41*, 43.

2. Yarin, A. L.; Zussman, E. *Polymer* **2004**, *45*, 2977.

3. Dzenis, Y. *Science* **2004**, *304*, 1917.

4. Beachley, V.; Wen, X. *Prog. Polym. Sci.* **2010**, *35*, 868.

5. He, X.; Xiao, Q.; Lu, C.; Wang, Y.; Zhang, X.; Zhao, J.; Zhang, W., Zhang, X.; Deng, Y. *Biomacromolecules* **2014**, *15*, 618.

6. Teh, T. K. H.; Toh, S. L.; Goh, J. C. H. *Tissue Eng. A* **2013**, *19*, 1360.

7. Amass, W.; Amass, A.; Tighe, B. *Polym. Int.* **1998**, *47*, 89.

8. Gupta, B.; Revagade, N.; Hilborn, J. *Prog. Polym. Sci.* **2007**, *32*, 455.

9. Savioli Lopes, M.; Jardini, A. L.; Maciel Filho, R. *Procedia Eng.* **2012**, *42*, 1402.

10. Wang, H. B.; Mullins, M. E.; Cregg, J. M.; Hurtado, A.; Oudega, M.; Trombley, M. T.; Gilbert, R. T. *J. Neural Eng.* **2009**, *6*, 016001.

11. Gümüşderelioğlu, M.; Dalkıranoğlu, S.; Aydin, R. S. T.; Çakmak, S. *J. Biomed. Mater. Res. A* **2011**, *98*, 461.

12. Whitaker, M. J.; Quirck, R. A.; Howdle, S. M.; Shakesheff, K. M. *J. Pharm. Pharmacol.* **2001**, *52*, 1427.

13. Lu, H.; Vo, J. M.; Chin, H. S.; Lin, J.; Cozin, M.; Tsay, R.; Eisig, S.; Landesberg, R. *J. Biomed. Mater. Res. A* **2008**, *86*, 1128.

14. Lu, Q.; Ganesan, K.; Simionescu, D. T.; Vyavahare, N. R. *Biomaterials* **2004**, *25*, 5227.

15. Chen, F. M.; Zhang, M.; Wu, Z. F. *Biomaterials* **2010**, *31*, 6279.

16. Sahoo, S.; Ang, L. T.; Goh, J. C. H.; Toh, S. L. *J. Biomed. Mater. Res. A* **2010**, *93*, 1539.

17. Jin, G.; Prabhakaran, M. P.; Kai, D.; Ramakrishna, S. *Eur. J. Pharm. Biopharm.* **2013**, *85*, 689.

18. Sell, S. A.; Wolfe, P. S.; Ericksen, J. J.; Simpson, D. G.; Bowlin, G. L. *Tissue Eng. A* **2011**, *17*, 2723.

19. Anitua, E. *Pract. Proced. Aesthet. Dent.* **2001**, *13*, 487.

20. Lubkowska, A.; Dolegowska, B.; Banfi, G. *J. Biol. Regul. Homeost. Agents* **2012**, *26*, 3S.

21. Horimizu, M.; Kawase, T.; Nakajima, Y.; Okuda, K.; Nagata, M.; Wolff, L. F.; Yoshie, H. *Cryobiology* **2013**, *66*, 223.

22. Anitua, E.; Sanchez, M.; Orive, G. *Adv. Drug Deliv. Rev.* **2010**, *62*, 741.

23. Lee, H. R.; Park, K. M.; Joung, Y. K.; Park, K. D.; Do, S. H. *J. Biomed. Mater. Res. A* **2012**, *100*, 3099.

24. Bir, S. C.; Esaki, J.; Marui, A.; Yamahara, K.; Tsubota, H.; Ikeda, T.; Sakata, R. *J. Vasc. Surg.* **2009**, *50*, 870.

25. Lu, H. H.; Vo, J. M.; Chin, H. S.; Lin, J.; Cozin, M.; Tsay, R.; Eisig, S.; Landesberg, R. *J. Biomed. Mater. Res. A* **2008**, *86*, 1128.

26. Nakajima, Y.; Kawase, T.; Kobayashi, M.; Okuda, K.; Wolff, L. F.; Yoshie, H. *Platelets* **2012**, *23*, 594.

27. Diaz-Gomez, L.; Alvarez-Lorenzo, C.; Concheiro, A.; Silva, M.; Dominguez, F.; Sheikh, F. A.; Cantu, T.; Desai, R.; Garcia, V. L.; Macossay, J. *Mater. Sci. Eng. C-Mater.* **2014**, *40*, 180.

28. Montini Ballarin, F.; Caracciolo, P. C.; Blotta, E.; Ballarin, V. L.; Abraham, G.A. *Mater. Sci. Eng. C-Mater.* **2014**, *42*, 489.

29. Khadka, D. B.; Hayne, D. T. *Nanomedicine NBM* **2012**, *8*, 1242.

30. Murphy, S. *Transfusion* **2005**, *45*, 634.

31. Pietramaggiori, G.; Kaipainen, A.; Czeczuga, J. M.; Wagner, C. T.; Orgill, D. P. *Wound Repair Regen.* **2006**, *14*, 573.

32. Zong, X.; Kim, K.; Fang, K.; Ran, S.; Hsiao, B. S.; Chu, B. *Polymer* **2002**, *43*, 4403.

33. Wang, W.; Barber, A. H. *J. Polym. Sci. Part B: Polym. Phys.* **2012**, *50*, 546.

34. Fouad, H.; Elsarnagawy, T.; Almajhdi, F. N.; Khalil, K. A. *Int. J. Electrochem. Sci.* **2013**, *8*, 2293.

35. Cui, W.; Li, X.; Zhu, X.; Yu, G.; Zhou, S.; Weng, J. *Biomacromolecules* **2006**, *7*, 1623.

36. Curgul, S.; Van Vliet, K. J.; Rutledge, G. C. *Macromolecules* **2007**, *40*, 8483.

37. Duan, Y.; Wang, Z.; Yan, W.; Wang, S.; Zhang, S.; Jia, J. *J. Biomater. Sci. Polym. Ed.* **2007**, *18*, 1153.

38. Berkland, C.; Pollauf, E.; Raman, C.; Silverman, R.; Kim, K.; Pack, D. W. *J. Pharm. Sci.* **2007**, *96*, 1176.

39. Jiang, H.; Hu, Y.; Zhao, P.; Li, Y.; Zhu, K. *J. Biomed. Mater. Res. B* **2006**, *79*, 50.

40. Nelson, P. J.; Daniel, T. O. *Kidney Int.* **2002**, *61*, S99.

41. Simamora, P.; Chern, W. *J. Drugs Dermatol.* **2006**, *5*, 436.

42. Anitua, E.; Andia, I.; Sanchez, M.; Azofra, J.; Zalduendo, M. M.; de la Fuente, M. *J. Orthop. Res.* **2005**, *23*, 281.

43. Baker, B. M.; Mauck, R. L. *Biomaterials* **2007**, *28*, 1967.

44. Prodanov, L.; Riet, J.; Lamers, E.; Domanski, M.; Luttge, R.; van Loon, J. J. W. A.; Jansen, J. A.; Walboomers, X. F. *Biomaterials* **2010**, *31*, 7758.

45. Shang, S.; Yang, F.; Cheng, X.; Walboomers, X. F.; Jansen, J. A. *Eur. Cells Mater.* **2010**, *19*, 180.

46. Teixeira, A. I.; Abrams, G. A.; Bertics, P. J.; Murphy, C. J.; Nealey, P. F. *J. Cell. Sci.* **2003**, *15*, 1881.

47. Whited, B. M.; Rylander, M. N. *Biotechnol. Bioeng.* **2014**, *111*, 184.